NASA Technical Memorandum 103928

77064
P.13

Laser-Spectroscopic Measurement Techniques for Hypersonic, Turbulent Wind Tunnel Flows

Robert L. McKenzie and Douglas G. Fletcher

March 1992

```
(NASA-TM-103928)   LASER-SPECTROSCOPIC              N92-19596
MEASUREMENT TECHNIQUES FOR HYPERSONIC,
TURBULENT WIND TUNNEL FLOWS  (NASA)  13 p
                                  CSCL 14B       Unclas
                                        G3/35   0077064
```

NASA
National Aeronautics and
Space Administration

Laser-Spectroscopic Measurement Techniques for Hypersonic, Turbulent Wind Tunnel Flows

Robert L. McKenzie and Douglas G. Fletcher, Ames Research Center, Moffett Field, California

March 1992

LASER-SPECTROSCOPIC MEASUREMENT TECHNIQUES FOR HYPERSONIC, TURBULENT WIND TUNNEL FLOWS

ROBERT L. MCKENZIE AND DOUGLAS G. FLETCHER
NASA Ames Research Center
Moffett Field, California, USA

1. Introduction

Until recently, aerodynamic measurements obtained away from a surface have been limited either to the use of intrusive probes to determine pressure, mass flux, and total temperature or to visualization methods for indications of the flow geometry. New laser-spectroscopic methods are now emerging which offer compelling opportunities to obtain simultaneous measurements of density, temperature, and their fluctuations, with unprecedented spatial and temporal resolution [1]. As a result, measurement techniques are now feasible which can be used in supersonic and hypersonic flows to characterize the effects of compressibility on turbulent behavior and to obtain quantitative descriptions of complex, three-dimensional flow fields.

Most of the laser-spectroscopic techniques incorporate laser-induced fluorescence (LIF) or Raman spectroscopy. The primary objective of this report is to describe the spectroscopic nature, present status, and capabilities of some LIF and Raman techniques which have been developed at NASA Ames Research Center. Particular emphasis has been centered on applications in hypersonic wind tunnels where measurements with more conventional probes are often inadequate or impractical. The requirements for laser-spectroscopic measurements in hypersonic flows are dictated by their intended aerodynamic research applications. By design, hypersonic flow fields over test articles are generally free of large stagnation regions. Consequently, in moderately heated facilities, they can have densities lower than 0.01 amagat and temperatures ranging from 50 K to 300 K. To provide sufficient sensitivity at the low temperatures, the spectroscopy must be based on individual rotational transitions in the interacting species. In addition, most applications are generally limited to chemically stable species which have been seeded into the flow or which occur naturally in air.

With these requirements in mind, two principal laser-spectroscopic approaches have been developed at NASA Ames Research Center for the measurement of temperature, density, and their fluctuations owing to turbulence in high-speed flows. Early work was centered on the use of near-ultraviolet lasers to induce fluorescence from trace concentrations of nitric oxide (NO) added to flows of nitrogen. More recently, advances in laser technology have allowed similar measurements to be made in unseeded air flows using vacuum-ultraviolet lasers to excite molecular oxygen.

2. Laser-Induced Fluorescence in Flows Containing Nitric Oxide

Prior to the availability of high-energy excimer lasers, a spectroscopic approach was developed which relied on the existing Nd:YAG-pumped, tunable dye laser technology. It was based a dual-frequency LIF technique in which two frequency-doubled dye lasers were each tuned to a near-ultraviolet, ro-vibronic transition in the Gamma Band spectrum of nitric oxide [2]. Pulse energies of 1 μJ could be achieved over the entire electronic band near 225 nm. The two independent, coincident LIF signals allowed density and temperature to be determined simultaneously. NO was added in concentrations of less than 100 ppm to a wind tunnel reservoir containing pure nitrogen. Because the NO fluorescence is quenched efficiently by oxygen and very little by nitrogen, the technique is most applicable in pure nitrogen flows.

The capabilities of the method were demonstrated in the turbulent boundary layer on the wall of a Mach-2 channel flow. Single-pulse measurements were obtained with a spatial resolution of less than 1 mm and uncertainties of less than 2%. A small blow-down wind tunnel was used which was designed to handle gas mixtures containing NO. Since NO is toxic in concentrations greater than 25 ppm, a test facility suitable for NO-LIF must incorporate all of the special features necessary to safely use toxic mixtures. Despite this inconvenience for general applications, the NO-LIF technique demonstrated the unique capabilities of laser-spectroscopic methods for aero-dynamic measurements. Its success encouraged investigations of similar techniques which could be applied to unseeded air flows.

3. Raman Scattering and Laser-Induced Fluorescence in Air Flows

3.1. BACKGROUND

The development of high energy, vacuum-ultraviolet, ArF excimer lasers made feasible the use of LIF from oxygen molecules in air. Exploration of the concept was initiated in 1981, before such lasers were available commercially, with a study solicited by NASA-Ames and performed by Massey and Lemon [3]. They were able to construct a tunable, ArF laser and demonstrate its use to obtain O_2 LIF signals in room air. Their measurements indicated that the LIF was sufficiently intense and sensitive to temperature to be a viable measurement technique in unseeded air flows.

The results of Massey and Lemon and the subsequent commercial availability of high-energy ArF excimer lasers encouraged further development of the concept. However, unlike the two-laser system used for NO-LIF, the cost and complexity of excimer lasers made the use of two lasers unattractive. Alternatively, Gross and McKenzie [4] proposed that both the fluorescence emission and the Raman scattering from each pulse of one laser be used to provide the two independent signals required for simultaneous temperature and density measurements. Since then, Laufer et al. have characterized the spectroscopy of O_2-LIF [5] and demonstrated its use to measure temperatures down to 130 K in a cell at known pressures [6]. The development was continued by Fletcher who incorporated the Raman signal to obtain simultaneous measurements of temperatures and densities, without knowledge of any other thermodynamic parameters [7]. Most recently, he has demonstrated the use of the O_2-LIF/Raman technique to measure temperature, density, and their fluctuations in the turbulent boundary layer of the same Mach-2 channel flow which was studied previously using NO-LIF [8].

3.2. O_2-LIF/RAMAN SPECTROSCOPY

The O_2 LIF process is characterized by the energy-level diagram shown in Fig. 1. The tuning range of the ArF laser is centered at 193.3 nm with a bandwidth of approximately 0.5 nm. Within that band, absorbing transitions may be accessed in the O_2 $B^3\Sigma_u^- \leftarrow X^3\Sigma_g^-$ Schumann-Runge band from $v'' = 0$ to $v' = 4,5$. Hot-band vibrational transitions are also accessible, including $v'' = 1$ to $v' = 7,8$; and $v'' = 2$ to $v' = 10,11,12$. In each vibrational band, the rotational transition pairs, P(K'') and R(K'' + 2), are at nearly the same frequency. The pairs associated with K'' = 15, 17, and 19 from $v',v'' = 4,0$ have been the principle absorbing transitions used for LIF at room temperature and below. Below room temperature, the population of levels with $v'' > 0$ is extremely small. However, the Frank-Condon factor for $v',v'' = 7,1$ transitions is 200 times greater than for $v',v'' = 4,0$ so that only a small population of the $v'' = 1$ level is necessary to produce observable hot-band absorption. The effect starts to become significant at temperatures slightly above 300 K.
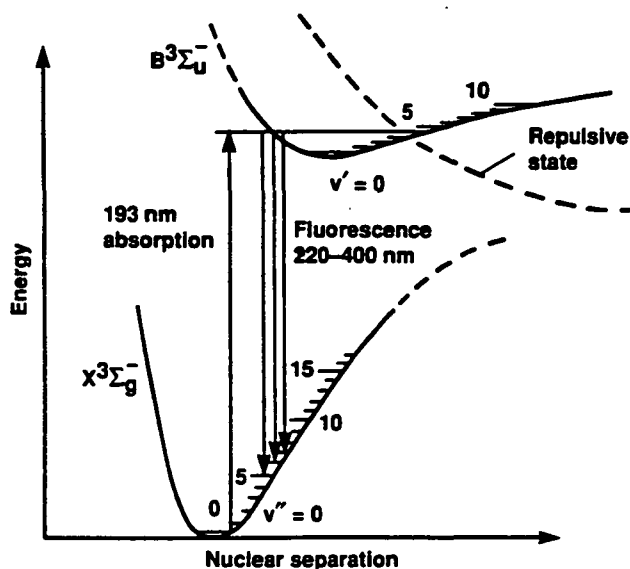

Figure 1. Energy-level diagram for O_2 laser-induced fluorescence by an ArF laser.

The $B^3\Sigma_u^-$ upper state of O_2 is crossed near the $v' = 4$ level by an array of repulsive states which are represented by a single curve in Fig. 1. Consequently, most molecules which are elevated to $v' \geq 4$ by the LIF process predissociate within a few picoseconds. The molecules that do not predissociate must have a radiative lifetime which is equally short. Consequently, it is much less than the time between molecular collisions at most wind tunnel test conditions. Collisional quenching effects on the LIF signals may then be neglected, thereby greatly simplifying the signal analysis required to determine temperature and density.

For fluorescence originating from $v' = 4$, the Franck-Condon factors favor spontaneous transitions back to all $X^3\Sigma_g^-$ vibrational levels above $v'' = 4$. The resulting fluorescence spectrum extends from 220 nm to greater than 400 nm. Although the total fluorescence signal is maximized if the entire band is observed, spectral interference from other laser-induced processes can limit the practical range of observation. In any case, at least half of the fluorescence energy is from wavelengths below 300 nm, which includes O_2 vibrational emission bands up to $v',v'' = 4,13$.

The LIF emission provides a signal which is sensitive to both temperature and density. The Raman signal can be made sensitive only to density. Taken together, the two contributions to the laser-induced spectrum allow temperature and density to be determined from each laser pulse.

An experimental spectrum of laser-induced radiation from air at room temperature is shown in Fig. 2. It was obtained using an optical multi-channel analyzer (OMA) at the exit plane of a small spectrometer with a 0.5-mm entrance slit. Because the image of the laser beam lies with its axis orthogonal to the slit, the slit width also determines the length of the observed sample volume. In this example, the spectral width of each feature is dominated by the width of the slit image. In addition, the grating has been positioned so that the contribution from Rayleigh scattering below 196 nm does not illuminate the OMA photo-diode array. The Δv notation refers to the overall change in vibrational quantum number resulting from the entire Raman or LIF process. The features denoted by $\Delta v = 1,2$ are the Raman fundamental and first overtone transitions of O_2. The Raman $\Delta v = 1$ transition from N_2 falls between them. The strengths of the O_2 Raman scattering are resonantly enhanced at 193 nm, which significantly improves the viability of Raman measurements in air at low densities. At room temperature and below, the fluorescence underlying the O_2 $\Delta v = 1$ Raman transition is negligible because the $v',v'' = 4,1$ Frank-Condon factor is so small. Hence, the $\Delta v = 1$ transitions of O_2 and N_2 may be assumed to result only from Q-branch Raman transitions for which all rotational components are at nearly the same frequency. The resulting, spectrally integrated signal is independent of temperature and is linearly proportional to the species density. The sum of O_2 and N_2 Raman contributions provide a maximum signal for determining the gas density. The Q_2 $\Delta v = 2$ feature is not included in the sum to avoid the small influence of underlying fluorescence.
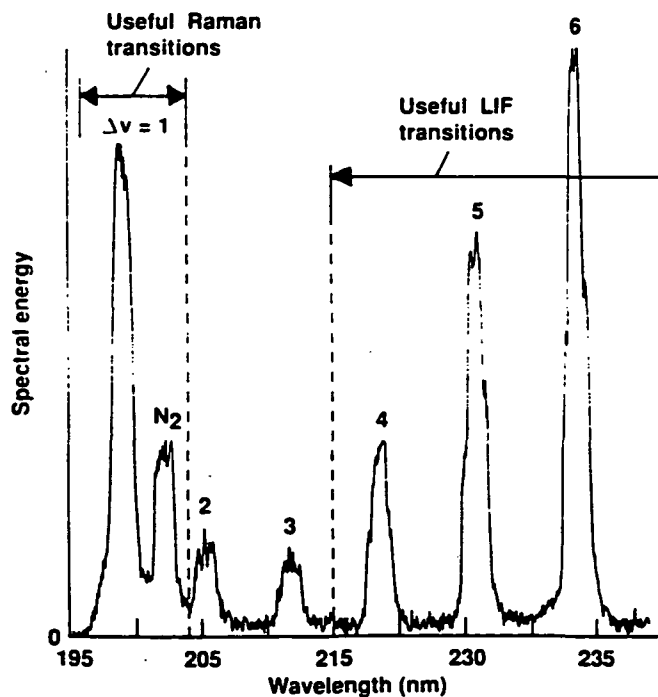

Figure 2. Emission spectrum from room air induced by an ArF laser with low fluence.

The LIF transitions at the wavelengths captured by the OMA diode array also appear in Fig. 2. The entire useful spectrum extends to $\Delta v = 13$ at 300 nm. The $\Delta v = 3$ transition is avoided because it contributes only a small fraction to the total fluorescence energy and includes a weak contribution from the second overtone of the resonance-enhanced O_2 Raman scattering.

Because the laser energy typically fluctuates ±5% from pulse to pulse, the Raman and LIF spectral energies for each pulse must be normalized by the corresponding laser energy. However, only the laser pulse energy can be measured accurately, but not its fluence (energy per unit area). Consequently, the observed radiative processes must be dominated by interactions for which the signal energies vary linearly with laser energy and are independent of the distribution of fluence within the beam cross section. The dominance of linear LIF processes depends both on the magnitude of laser fluence and on its wavelength. For example, Fig. 3 shows that as the laser fluence exceeds about 1.5 J/cm^2, both the Raman and LIF energy behave quadratically, depending on the transition excited. This behavior is the consequence of underlying multi-photon processes with excitation rates that increase non-linearly with laser fluence and become dominant at high values.
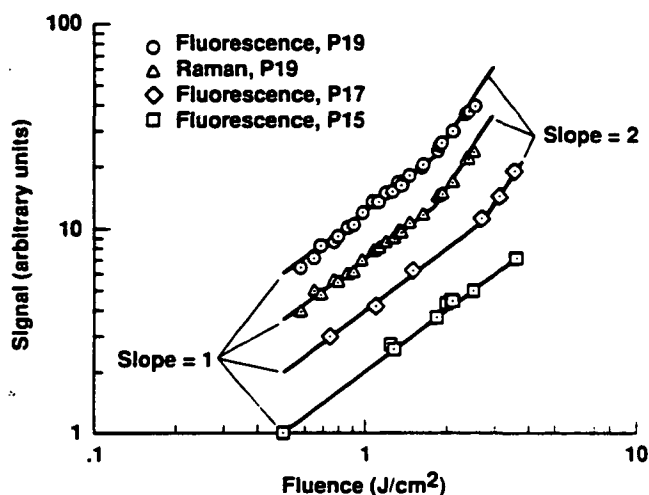

Figure 3. Dependence of total fluorescence and Raman signals on the spatially-averaged fluence of a narrowband ArF laser. (Note: The signal magnitudes for each case have been arbitrarily separated for clarity.)

The dependence of the non-linear processes on laser wavelength is demonstrated more explicitly in Fig. 4. It shows an excitation spectrum in which the total LIF energy is monitored while the laser is tuned through the absorbing O_2 transitions. The laser has been focused to achieve a high average fluence. The non-linear resonances, denoted by asterisks, do not appear when an unfocused beam of the same pulse energy is used. Most of them have been identified as resonances associated with the photoion, O_2^+. The resonant wavelengths of the non-linear processes influence the choice of O_2 transitions used to obtain LIF measurements. For example, the P19 and R21 transitions are both strongly affected. Interference underlying the Raman transitions also occurs at this laser wavelength, as shown by Fig. 3. The P17 transition can be affected similarly if the laser is not carefully tuned or sufficiently narrowband. The nearby R19 transition produces weaker LIF signals than those from P17 but lies farther from the non-linear resonance. Finally, the P15 transition is apparently free of nearby non-linear resonances for the range of fluence investigated.
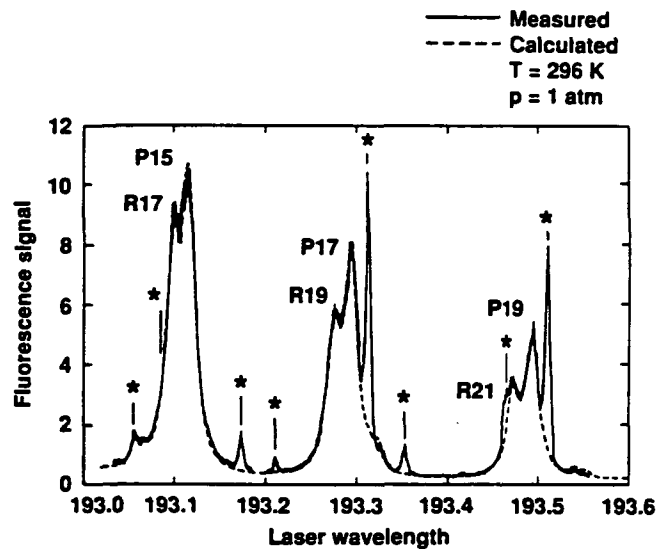
Figure 4. Oxygen excitation spectrum stimulated by a focused laser beam with an average fluence of about 1.5 J/cm^2. Multi-photon transitions are denoted by asterisks.

3.3. APPLICATION TO A MACH-2 TURBULENT BOUNDARY LAYER

Work is now in progress to demonstrate the use of the O_2-LIF/Raman technique for simultaneous measurements of temperatures, densities, and their fluctuations owing to supersonic turbulence [8]. The characteristics of the test flow have been described previously [2-3]. It includes a 12.1-mm thick, fully turbulent boundary layer that is adjoined by a relatively undisturbed flow of the same thickness.

In Fig. 5, the average temperature and density profiles obtained from O_2-LIF/Raman data are compared with distributions implied from pressure measurements using a pitot probe and a static pressure port in the wall below the sample volume. Spatial resolution of the spectroscopic measurements was about 1 mm. Agreement of comparable data is within $\pm 3\%$. Since the flow is in thermochemical equilibrium and both state variables have been measured simultaneously, the O_2-LIF/Raman data may also be used in conjunction with the equation of state to determine the local pressure. The pressure distribution is nearly constant, as expected for a flat-wall boundary layer. These results are identical to those obtained previously using NO-LIF.

Figure 6 shows a comparison of the root-mean-square (rms) fluctuation amplitudes of temperature and density obtained from both spectroscopic methods and from hot-wire data. Again, the NO-LIF and O_2-LIF/Raman results are in agreement. They both show a region in the boundary layer near $Y/\delta = 0.6$ where the density fluctuations are exceptionally large. A histogram of the NO-LIF fluctuations displays a bimodal character which suggests that a weak wave was oscillating across the sample volume. Such density fluctuations also imply the presence of pressure fluctuations in that region. On the other hand, an analysis of the hot-wire signals to obtain density fluctuations requires the assumption that pressure fluctuations are negligible. Clearly, that is not the case in this flow and the effects of pressure fluctuations would not have been observed without the use of the LIF instrumentation. These comparisons demonstrate that

the O_2-LIF/Raman technique can provide accurate measurements in air flows at the low temperatures and densities which are prevalent in high-speed wind tunnels.
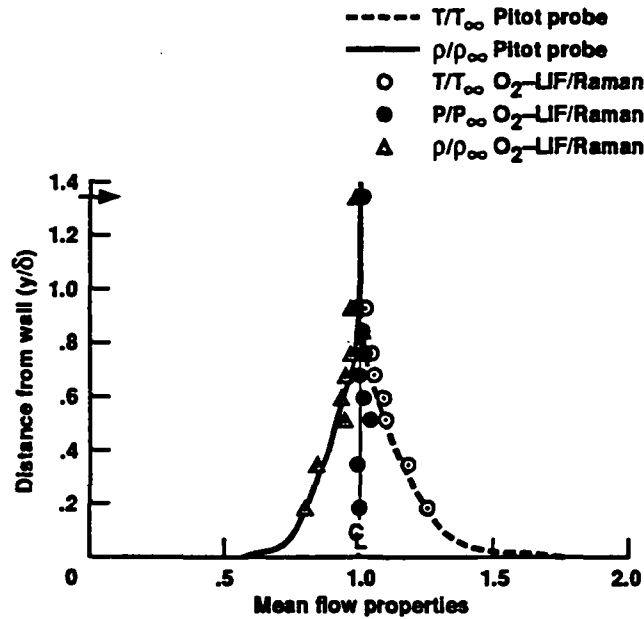

Figure 5. Time-averaged temperature, density, and pressure distributions in a turbulent boundary layer with a centerline Mach number $M_\infty = 2.06$, stream temperature $T_\infty = 158$ K, stream pressure $P_\infty = 0.35$ atm, and thickness $\delta = 12.1$ mm. Local values are normalized by their respective free stream values.
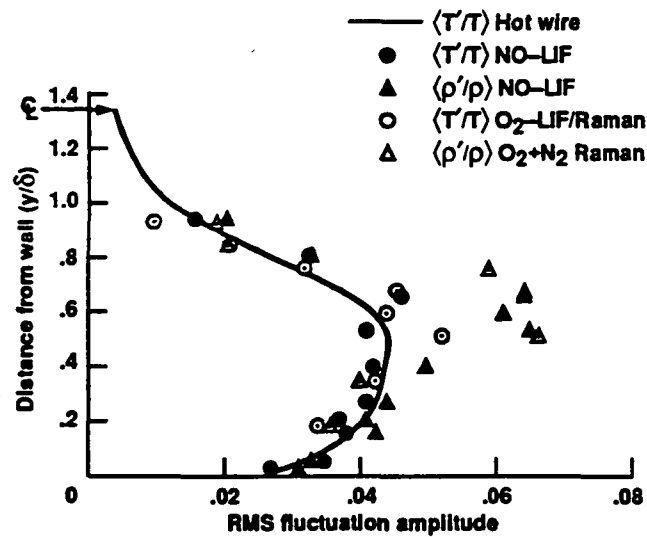

Figure 6. Comparisons of temperature and density rms-fluctuation amplitudes obtained with LIF techniques or implied by hot-wire anemometer data. Flow conditions are the same as in Fig. 5. For each variable, the fluctuation amplitude is normalized by the local time-averaged value.

4. Applications to Large-Scale Hypersonic Flows

A compelling application of the O_2-LIF/Raman technique is to flows in the NASA-Ames 3.5 ft. Hypersonic Wind Tunnel. Its test region is a open free-jet at Mach numbers of 5, 7,and 10, depending on the nozzle. The test environment serves as a relevant example for evaluations of the capabilities of O_2-LIF/Raman techniques.

LIF measurements have been demonstrated in which uncertainties greater than 1% may be characterized solely by the unavoidable effects of photon-statistical noise in the radiative signals [6]. In that case, the uncertainty or rms-noise/signal ratio for pulsed signals is simply equal to $[n_e]^{-1/2}$, where n_e is the average number of photo-electrons detected per pulse. This feature allows the corresponding uncertainties in temperature and density to be predicted in terms of the laser pulse energy and the efficiencies of the detector and collection optics. It may also be used to extend predictions based on the design parameters chosen used here to other values of pulse energy, f-number, etc.

For a given temperature, the weakest LIF signals are always obtained at the lowest densities. The density, $\rho = 0.02$ amagat, is representative of the free-stream density at Mach 7. To evaluate the capabilities of O_2-LIF/Raman measurements, the corresponding uncertainties in temperature measurement may be calculated using the most favorable set of optical parameters believed achievable and assuming that the optical system accepts fluorescence emission from all upper states with $\Delta v \leq 11$. In practice, more restrictive filtering of the emission spectrum may be required, depending on the experimental arrangement.

Among the significant parameters related to the performance of the collection optics system are its effective f-number and the transmission and reflection losses of its optical components. A system design based on f/2 optics, for which only 1.5% of the total radiative emission is collected, will still require a large device to match the focal lengths necessary in a large-scale facility. For example, in the Ames hypersonic facility, the optics can not be much closer to the flow centerline than 1 m, thereby requiring an f/2 system to have an aperture diameter of 50 cm. If a Cassegrain telescope is used, its two mirrors typically provide a combined reflectivity of 75% at 200 nm. In addition, the mirrors must be protected from heat and dust from the free-jet flow by several window panes of fused silica. Their combined transmission, including absorption and surface reflection losses, will be near 60%. Finally, isolation of the Raman spectra requires a monochromator with at least a grating, even if all other mirrors are eliminated. Grating efficiencies near 200 nm are typically less than 50%. Finally, losses at the monochromator entrance slit owing to imperfect imaging can exceed 10%. Thus, an overall transmission of no better than 20% should be expected. This value, combined with the collection efficiency of f/2 optics and a representative detector quantum efficiency of 12%, leads to an anticipated efficiency for conversion of emitted photons to detected photoelectrons of only 1/3000.

The laser pulse used for the calculations has been limited to 15 mJ, to stay within the range of fluence for linear behavior with a 1-mm spatial resolution at all laser wavelengths. However, linear behavior has been demonstrated for excitation of the P15 transition with pulse energies to 30 mJ, as Fig. 3 indicates.

The effect of the Raman signal uncertainty is also included in the temperature uncertainty calculation since the LIF signals are proportional to density. For the parameters given, the density measurements will contain a 5% rms-uncertainty owing to photon-statistical noise. However, density fluctuations owing to turbulence at hypersonic speeds are expected to be larger.

The variations in temperature measurement uncertainty are shown in Fig. 7 for narrowband laser wavelengths which are resonant with the absorbing transitions indicated. At the lowest

temperatures, the P15 transition is superior and can be further enhanced in practice by using higher pulse energies. However, its useful range of temperatures is limited and superseded by the R19 transition above 140 K. The P17 transition is not attractive at low temperatures because it is most favorable in only a limited temperature range and susceptible to non-linear interference. Above 300 K, the sensitivity of any v',v" = 4,0 transition must be compared with that available from excitation of the hot-band v',v" = 7,1 transitions [6].
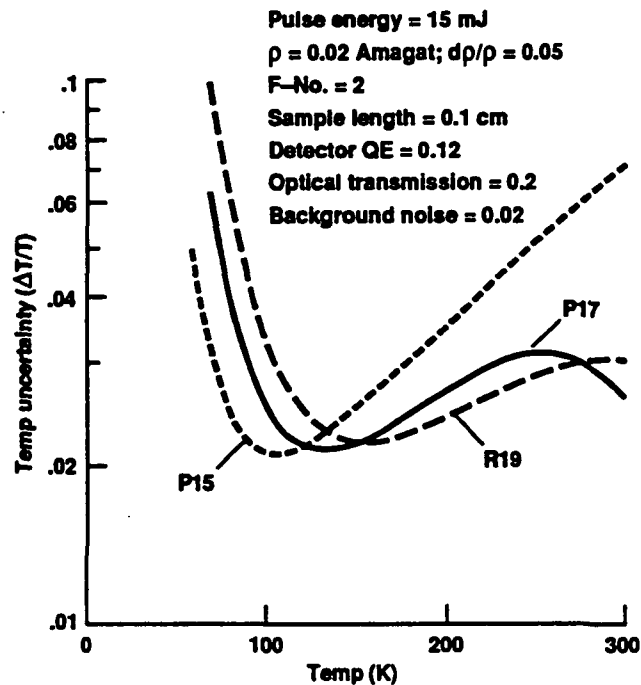

Figure 7. Predictions of temperature measurement uncertainties owing to photon-statistical noise for constant density and laser pulse energy.

5. Conclusions

These results demonstrate that laser-spectroscopic techniques can be used to obtain measurements of temperature, density, and their turbulent fluctuations and they show the feasibility of using a carefully tuned, narrowband ArF excimer laser and O_2-LIF/Raman spectroscopy to measure temperatures and densities at hypersonic wind tunnel conditions with uncertainties of less that 5%.

6. References

1. McKenzie, R. L. (1991) "Progress in Laser-Spectroscopic Techniques for Aerodynamic Measurements—An Overview," AIAA Paper 91-0059.

2. Gross, K. P., McKenzie, R. L., and Logan, P. (1987) "Measurements of Temperature, Density, Pressure, and Their Fluctuations in Supersonic Turbulence Using Laser-Induced Fluorescence," Exp. in Fluids, 5, pp. 372-380.

3. Massey, G. A. and Lemon, C. J. (1984) "Feasibility of Measuring Temperature and Density Fluctuations in Air Using Laser-Induced O_2 Fluorescence," IEEE Journ. Quantum Elect., QE-20, pp. 454-457.

4. Gross, K. P. and McKenzie, R. L. (1985) "Optical Diagnostics of Unseeded Turbulent Flows Using Ultraviolet Laser-Induced Processes in Air," Unpublished Research Proposal.

5. Laufer, G., McKenzie, R. L., and Huo, W. M. (1988) "Radiative Processes in Air Excited by an ArF Laser," Optics Lett., 13, pp. 99-101.

6. Laufer, G., McKenzie, R. L., and Fletcher, D. G. (1990) "Method for Measuring Temperatures and Densities in Hypersonic Wind Tunnel Air Flows Using Laser-Induced O_2 Fluorescence," Applied Optics, 29, pp. 4873-4883.

7. Fletcher, D. G. and McKenzie, R. L. (1991) "Simultaneous Measurements of Temperature and Density in Air Flows Using UV Laser Spectroscopy," AIAA Paper 91-0458.

8. Fletcher, D. G. (1992) "Measurements of Density, Temperature, and Their Fluctuations in Turbulent, Supersonic Flow Using UV Laser Spectroscopy," Unpublished presentation at the AIAA 30th Aerospace Sciences Meeting, Reno, NV.

REPORT DOCUMENTATION PAGE

Public reporting burden for this collection of information is estimated to average 1 hour per response, including the time for reviewing instructions, searching existing data sources, gathering and maintaining the data needed, and completing and reviewing the collection of information. Send comments regarding this burden estimate or any other aspect of this collection of information, including suggestions for reducing this burden, to Washington Headquarters Services, Directorate for Information Operations and Reports, 1215 Jefferson Davis Highway, Suite 1204, Arlington, VA 22202-4302, and to the Office of Management and Budget, Paperwork Reduction Project (0704-0188), Washington, DC 20503.

1. AGENCY USE ONLY (Leave blank)	2. REPORT DATE March 1992	3. REPORT TYPE AND DATES COVERED Technical Memorandum

4. TITLE AND SUBTITLE

Laser-Spectroscopic Measurement Techniques for Hypersonic, Turbulent Wind Tunnel Flows

6. AUTHOR(S)

Robert L. McKenzie and Douglas G. Fletcher

5. FUNDING NUMBERS

505-59-40

7. PERFORMING ORGANIZATION NAME(S) AND ADDRESS(ES)

Ames Research Center
Moffett Field, CA 94035-1000

8. PERFORMING ORGANIZATION REPORT NUMBER

A-92076

9. SPONSORING/MONITORING AGENCY NAME(S) AND ADDRESS(ES)

National Aeronautics and Space Administration
Washington, DC 20546-0001

10. SPONSORING/MONITORING AGENCY REPORT NUMBER

NASA TM-103928

11. SUPPLEMENTARY NOTES

Point of Contact: Robert L. McKenzie, Ames Research Center, MS 229-1, Moffett Field, CA 94035-1000; (415) 604-6158 or FTS 464-6158

12a. DISTRIBUTION/AVAILABILITY STATEMENT

Unclassified — Unlimited
Subject Category 35

12b. DISTRIBUTION CODE

13. ABSTRACT (Maximum 200 words)

A review is given of the nature, present status, and capabilities of two laser-spectroscopic methods for the simultaneous measurement of temperature, density, and their fluctuations owing to turbulence in high speed wind tunnel flows. One method is based on the two-frequency excitation of nitric oxide seeded into a nitrogen flow, using tunable dye lasers. The second, more recent method relies on the excitation of oxygen in air flows using a tunable, ArF excimer laser. Signals are obtained from both the laser-induced fluorescence and from Raman scattering of the same laser pulse. Measurements are demonstrated in the turbulent boundary layer of a Mach-2 channel flow.

14. SUBJECT TERMS
Hypersonic flow measurements, Turbulent flow measurements, Laser-induced fluorescence, Flow diagnostics, Oxygen fluorescence, Temperature measurements, Density measurements

15. NUMBER OF PAGES
14

16. PRICE CODE
A02

17. SECURITY CLASSIFICATION OF REPORT	18. SECURITY CLASSIFICATION OF THIS PAGE	19. SECURITY CLASSIFICATION OF ABSTRACT	20. LIMITATION OF ABSTRACT
Unclassified	Unclassified		